Bioelectrochemistry 139 (2021) 107744

Contents lists available at ScienceDirect

Bioelectrochemistry

journal homepage: www.elsevier.com/locate/bioelechem

The electrochemical immunosensor for detection of prostatic specific antigen using quince seed mucilage-GNPs-SNPs as a green composite

Elahe Darvishi [a], Hosna Ehzari [b], Mohsen Shahlaei [b], Leila Behbood [a], Elham Arkan [a,*]

[a] Nano Drug Delivery Research Center, Health Technology Institute, Kermanshah University of Medical Sciences, Kermanshah, Iran
[b] Pharmaceutical Sciences Research Center, Health Institute, Kermanshah University of Medical Sciences, Kermanshah, Iran

ARTICLE INFO

Article history:
Received 29 August 2020
Received in revised form 9 January 2021
Accepted 12 January 2021
Available online 18 January 2021

Keywords:
Electrochemical impedance spectroscopy
Quince seed mucilage
Gold and silver nanoparticles
Green synthesis
Biomarkers

ABSTRACT

Prostatic specific antigen (PSA) is known as a biomarker of prostate cancer. In males, prostate cancer is ranked second as leading cause of death out of more than 200 different cancer types1. As a result, early detection of cancer can cause a significant reduction in mortality. PSA concentration directly is related to prostate cancer, so normal serum concentrations in healthy means are 4 ng and above 10 ng as abnormal concentration. Therefore, PSA determination is important to cancer progression. In this study, a free label electrochemical immunosensor was prepared based on a new green platform for the quantitative detection of the PSA. The used platform was formed from quince seed mucilage containing green gold and silver nanoparticles and synthesized by the green method (using *Calendula officinalis L.* extract). The quince mucilage biopolymer was used as a sub layer to assemble nanoparticles and increase the electrochemical performance. This nanocomposite was used to increase the antibody loading and accelerate the electron transfer, which can increase the biosensor sensitivity. The antibodies of the PSA biomarker were successfully incubated on the green platform. Under the optimal conditions, the electrochemical impedance spectroscopy (EIS) was proportional to the PSA biomarker concentration from 0.1 pg mL^{-1} to 100 ng mL^{-1} with low limit of detection (0.078 pg mL^{-1}). The proposed green immunosensor exhibited high stability and reproducibility, which can be used for the quantitative assay of the PSA biomarker in clinical analyses. The results of real sample analysis presented another tool for the PSA biomarker detection in physiologic models.

1. Introduction

One of the most prevalent cancers is prostate cancer all around the world (1.31 per people), which is the second typical cancer between men following skin cancers [1]. Early diagnosis of prostate cancer is of particular importance in reducing mortality [2]. One of the effective methods for diagnosis and treatment of the disease is the diagnosis of its biological markers. Currently, the best biomarker for controlling and detecting prostate cancer is a prostatic specific antigen (PSA). PSA is a serine protease formed from 93% peptide and 7% sugar. In the monomer structure, this antigen has 240 amino acids and four carbohydrate side chains. PSA is secreted by both healthy and prostate gland cancer cells [3]. The normal level of PSA in human blood, 0.4 ng ml^{-1}, increases several times in prostate cancer. About 30% of men with a PSA level ranging from 4.1 to 9.9 ng ml^{-1} suffer from the disease [4]. Therefore, accurate measurement of PSA levels in the bloodstream is one of the main factors concerning the diagnosis and treatment of prostate cancer.

To date, important studies have been carried out on developing sensitive, precise, rapid, and selective sensors for rapid diagnosis of cancer. The electrochemical immunosensor are analytical devices with high selectivity and sensitivity. Electrochemical immunosensors are easier and more portable than other analytical instruments [5]. Moreover, they can perform in situ or automatic detection. Antibodies are normally immobilized on the surface of different transformers [6]. Antibodies could be specifically targeted to anti-cancer biomarkers. They have the potential to identify antigens in a medical clinic. The signals produced by the electrochemical transducers can be voltammetric, potentiometric, conductometric, or impedimetric [7].

Today, due to the unique properties of nanoscale materials, nanotechnology has become more important, and has extensive applications in the sensors, medical and pharmaceutical industries, electronics, and agriculture [8–10]. In the last decades, nanomaterial has been considered regarding the chemical, physical, and biological properties to electrochemical sensors fabrication. Gold

* Corresponding author.
E-mail address: e.arkan@kums.ac.ir (E. Arkan).

https://doi.org/10.1016/j.bioelechem.2021.107744
1567-5394/

nanoparticles)GNPs) are of high conductivity, high surface area, and excellent biocompatibility. Furthermore, they provide sites with high absorption for antibody bonding and protect the antibody biological function. However, changes in the GNPs temperature and pH conditions lead to their aggregation [11].

Quince seed mucilage was used as a sub layer for assemble of gold and silver nanoparticles. It is a promising candidate for immobilization of nanoparticles owing to its significant mechanical strength, high surface area, excellent chemical stability, and high ability for immobilization of different mediators.

In addition, the above-mentioned nanocomposite increases the antibody loading and accelerates the electron transfer. It could also increase the biosensor sensitivity [12–14]. The chemical methods for synthesis of nanoparticles, such as grinding and condensing steam are used today. Harmful chemicals and toxicity and the environmental damage caused by them have created a lot of concerns [15]. Therefore, the extracts of different plants were used for synthesis of biocompatible nanoparticles and have attracted a great deal of scientific attention in the recent years [16]. The advantages of the green method include non-toxicity, biocompatibility, low cost, and the production of high-purity nanoparticles [17]. The green nanoparticles could be utilized in biological applications, sensors for instance [18]. In the plant extracts, there are various compositions, such as reducing, stabilizing, and covering agents used for the preparation of nanoparticles. Green synthesized gold and silver nanoparticles are suitable for binding of the PSA to be used in label-free electrochemical immunosensor owing to the presence of several functional groups around them. Additionally, they are safe, biocompatible, and environmentally friendly.

Cydonia oblonga Miller is a plant from the Rosacea family grown in certain parts of Asia, including Iran. Quince seed Mucilage, also known as a biopolymer, has several applications in the pharmaceutical industry [19,20]. It is used as an adjuvant in the manufacturing of different pharmaceutical dosage forms, including binding, thickening, stabilizing, humidifying, disintegrating, suspending, and emulsifying at different proportions. Quince seed mucilage comprises different components, such as cellulose and water-soluble polysaccharide, [21]. Herein, quince seed mucilage biopolymer was used as a layer to hold the nanoparticles for the modification of electrode surface because of its specific polymeric structure. In addition, it could be employed to increase the efficiency of electrode and to prepare biosensor with high detection capability due to the presence of different bioactive compounds in this mucilage and its negative charge.

Calendula officinalis L. has a considerable number of medical compounds [22]. The *Calendula* extract and its secondary metabolites could be used for the preparation of nanoparticles like gold and silver nanoparticles by reducing metal ions.

In the present study, a sensitive green free-labeled electrochemical immunosensor was designed for the determination of PSA in human blood. In the construction of the immunosensor, the quince seed mucilage was utilized to assemble gold and silver nanoparticles (GNP and SNP). The gold and silver nanoparticles were synthesized with the green method and their unique properties were used in the sensor platform (see Scheme 1).

2. Experimental

2.1. Reagents and chemicals

All Materials and reagents were obtained as analytical grade and used without additional purification. Hydrogen tetrachloroaurate tetrahydrate ($HAuCl_4{\cdot}4H_2O$), $AgNO_3$, Potassium ferrocyanide ($K_4Fe(CN)_6$), potassium ferricyanide ($K_3Fe(CN)_6$, N-ethyl-N′-(3-di methylaminopropyl) carbodiimide hydrochloride (EDC), N-hydroxysuccinimide (NHS), potassium ferricyanide and ferrocyanide salts were acquired from Sigma–Aldrich Co. (Munich, Germany). Bovine serum albumin (BSA), PSA antibody (anti-PSA) and PSA antigen were prepared from Biogen. Calendula officinalis L. and quince (Cydonia oblanga miller) seed were collected from Kermanshah-Iran. Phosphate buffer solution (PBS) (0.1 M) at pH = 7 was prepared by 0.1 M of potassium dihydrogen phosphate (KH_2PO_4). KH_2PO_4 and potassium chloride (KCl) were purchased

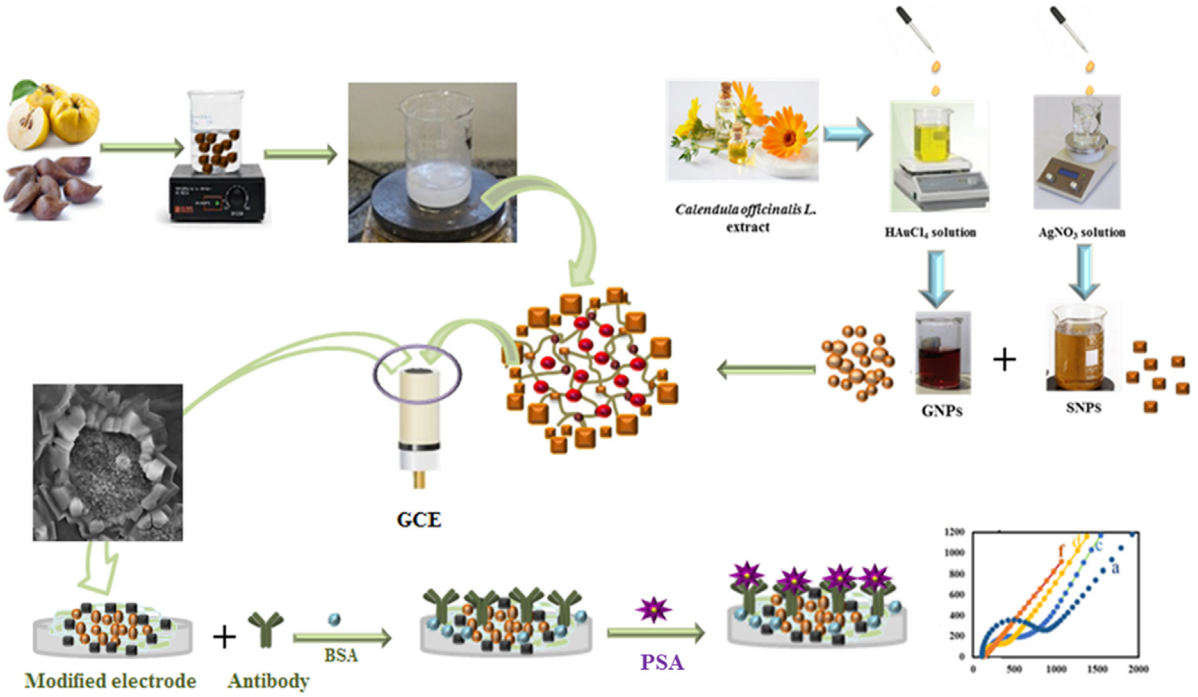

Scheme 1. The schematic illustration from the preparation process of green electrochemical immunosensor.

from the Merck Co. of Germany. Double distilled water was used for preparation aqueous solutions.

2.2. Apparatus

An Autolab system potentiostat–galvanostat model PGSTAT 204 (Utrecht, The Netherlands) using a NOVA (1.11) software was exerted to all of the electrochemical experiments which were carried out at room temperature. A silver-silver chloride (Ag/AgCl, saturated KCl) electrode and a platinum wire were utilized as reference and auxiliary electrodes, respectively. The EIS with the FRA 32 impedance analysis module, and the CV experiments were performed by mucilage-GNPs-SNPs/GCE as a working electrode. The EIS measurements were done in $Fe(CN)_6^{3-/4-}$ solution (0.5 mM) as the redox probe. A 5 mV amplitude AC voltage and frequency range from 10 kHz to 0.01 Hz were applied to the device under open-circuit potential (OCP). Metrohm pH-meter, Model 691, equipped with a glass electrode was applied during the experiments. To evaluation the manufactured surface morphology analysis, the methods of scanning electron microscope (SEM) (Philips XL 30) and Energy-dispersive X-ray spectroscopy (EDX) were employed. In these experiments, the EURONDA (EUROSONIC 4D model) was utilized to disperse the particles inside the solution and its uniformity.

2.3. Green synthesis of nanoparticles

2.3.1. Plant extracts preparation

To prepare plant extract, *Calendula officinalis L.* flowers were dried at room temperature. 2 gr of flowers powder dispersed in the 100 ml of distilled water was heated for 5 min at 100 °C. Then the *Calendula* extract was centrifuged at 8000 rpm for 15 min. Finally, the precipitate was removed and the extract was stored at 4 °C.

2.3.1.1. Green synthesis of GNPs. For green synthesis of gold nanoparticles, tetrachloroauric acid ($HAuCl_4$) solution (1 mM) was prepared and was heated to boiling temperature. The ratio 1:5 of *Calendula* extract and $HAuCl_4$ solution were mixed under constant stirring. After 2 min, the color of reaction mixture became red owing to the synthesis of gold nanoparticles. Then, the mixture was centrifuged at 10000 rpm for 10 min at 4 °C. The red precipitate was washed with distilled water twice and dried.

2.3.1.2. Green synthesis of SNPs. For green synthesis of silver nanoparticles, silver nitrate ($AgNO_3$) solution (1 mM) was prepared. The ratio 1:5 of *Calendula* extract was added to silver nitrate solution and was kept for 24 h under constant stirring. The color change of the reaction mixture confirmed the synthesis of silver nanoparticles. Then the mixture was centrifuged at 10000 rpm for 10 min at 4 °C. The precipitate was washed with distilled water twice and kept in dark place at 4 °C.

2.3.1.3. Characterization of nanoparticles. The nanoparticles were characterized by SEM microscopy, UV–Visible spectroscopy and FT-IR spectroscopy. Also size and surface charge of GNPs and SNPs were determined by zeta sizer.

2.4. Preparation of quince seed mucilage

Dried quince seeds were immersed into distilled water (at quince seeds/ water ratio of 1 gr: 25 cc) overnight. The solution

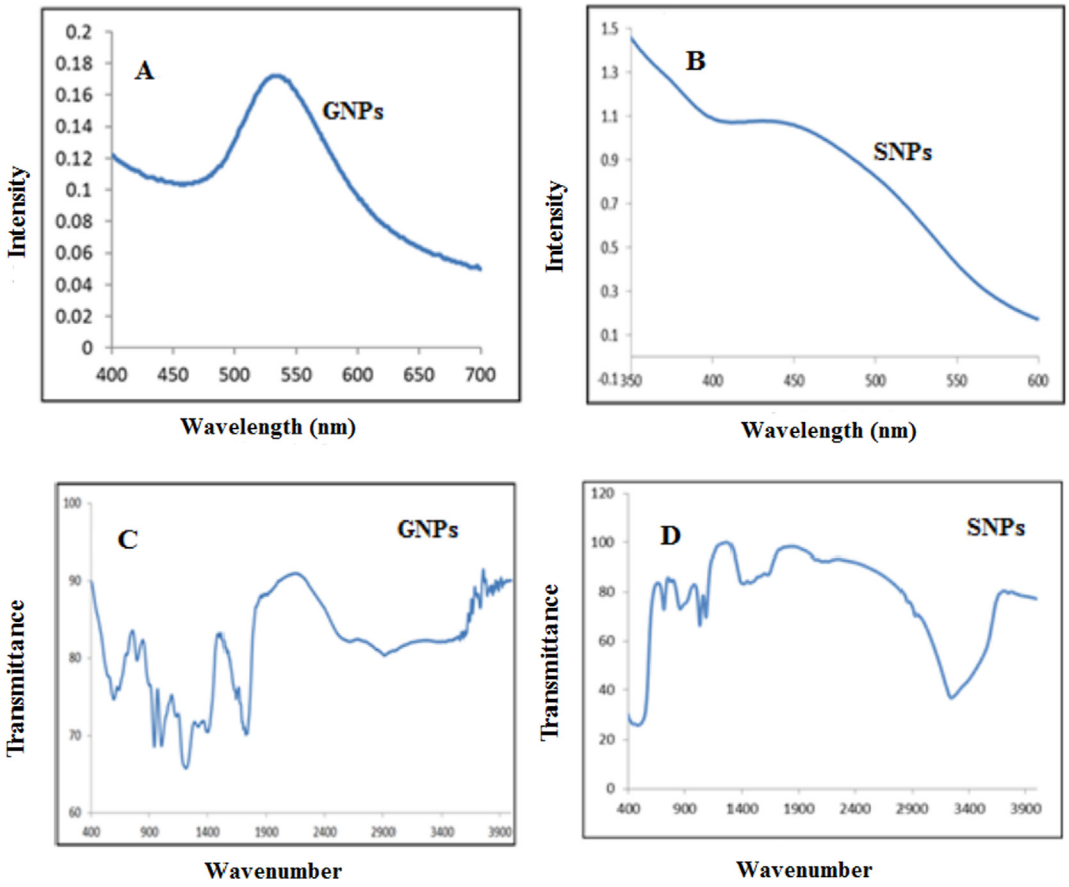

Fig. 1. Characterization of GNPs and SNPs.

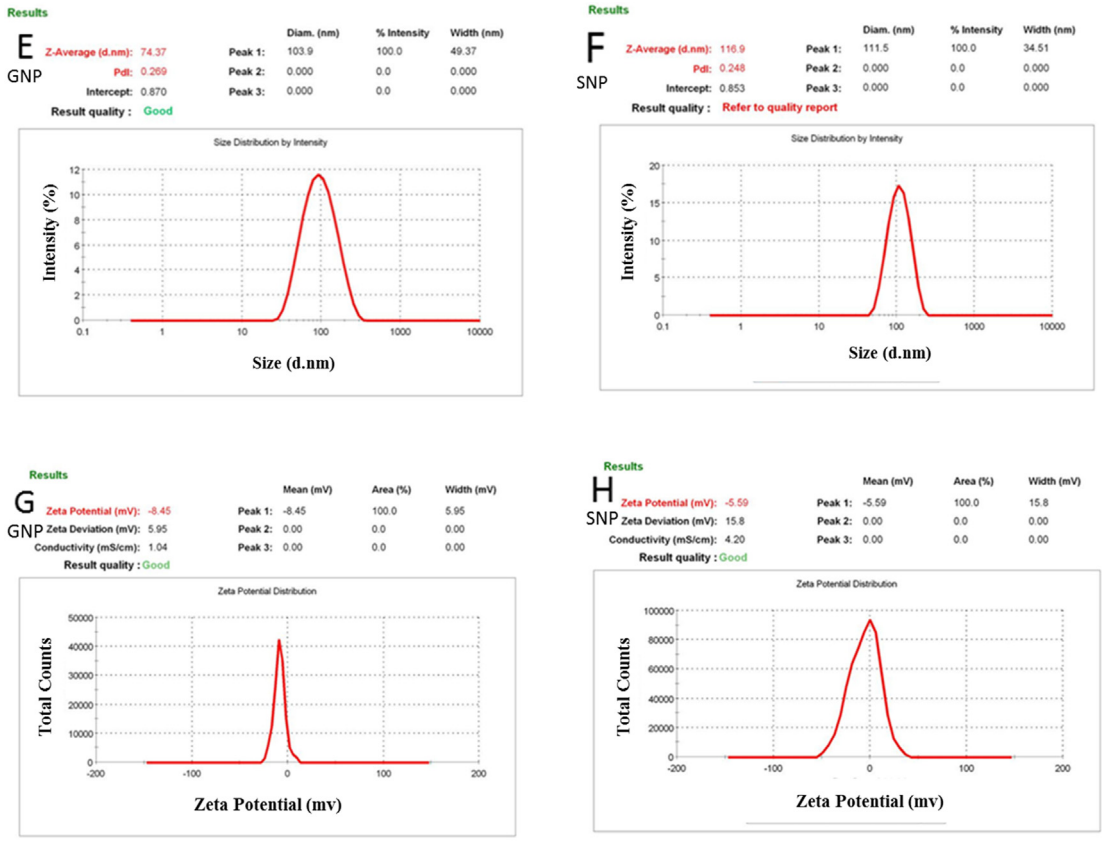

Fig. 1 (*continued*)

was filtered by cotton gauze to remove seeds and impurities. Then ethanol %96 was added to precipitate mucilage and removed impurities. The extracted mucilage was dried at 60°C overnight. Then the solution of mucilage (%2) was prepared to use as assembling agent for nanoparticles and antibodies on the surface of electrode.

2.5. Preparation of the immunosensor

In the present study, mucilage-GNPs-SNPs composite was applied as the electrode substrate to improve the electrode specific surface area and increase the PSA antibody immobilization and the electrochemical efficiency of the electrode. PSA antibody (contains N-H functional group at its end) was immobilized on the electrode because there is many carboxyl groups in quince seed mucilage and on the surface of GNPs and SNPs. To preparation of mucilage-GNPs-SNPs composite, 1 μL of mucilage %1, 1 μL of GNPs and 1 μL of SNPs solution were mixed. Then the solution was diluted to 1 ml volume.

The surface of bare GCE (i.d.¼3.0 mm, Azar Electrode, Urmia, Iran) was cleaned by polishing on a canton cloth with 0.3, 0.1 and 0.05 mm Al_2O_3 slurry and washed with double distilled water. Then the electrode was placed in water–ethanol solution (1:1) and the electrode was placed in an ultrasonic bath for 20 min to be completely clean and shiny. In the next step, 5 μL of the prepared mucilage-GNPs-SNPs composite was incubated on the surface of the GCE and it was dried at room temperature. Then, the electrode was immersed in 0.01 M PBS of pH = 7.0 containing 20 mM EDC and 40 mM NHS for 45 min to activate the carboxylic groups at the mucilage-GNPs-SNPs/GCE. The electrode was then washed with PBS. Then, a 10 μL of Ab (with the concentration of 15 μg/ml) was dropped onto the modified electrode surface and dried at room temperature, after waiting, excess Ab were removed by the buffer. The mentioned procedure was repeated three times. Afterwards, 4.0 μL of 1% BSA solution for 30 min was incubated onto the electrode to eliminate nonspecific adsorption. Eventually, the electrode (denoted as Ab/mucilage-GNPs-SNPs/GCE) was rinsed with deionized water, dried in air and stored at 4 °C in 0.1 M PBS of pH 7 when not in use. The solution of the PSA with varying concentrations was incubated onto Ab/mucilage-GNPs-SNPs/GCE surface and kept for 60 min at room temperature, and then it was washed by PBS to remove unbounded PSA. The prepared electrode was stored at 4 °C prior for further use. The electrochemical measurements of the immunosensor were performed in solution of a 0.1 M PBS (pH = 7.0) with 0.5 mM $[Fe(CN)_6]^{3-/4-}$ by DPV and CVs method.

3. Results and discussion

3.1. Characterization of GNPs and SNPs

Characterization of GNPs and SNPs were performed. UV–Vis spectrum of GNPs and SNPs confirm the green synthesis of nanoparticles (A and B). The FTIR of nanoparticles confirm the presence of several functional groups (C and D). The hydrodynamic average size of nanoparticles (E and F). Zeta potential of nanoparticles (G and H).

UV–Vis spectroscopy was used to confirm the green synthesis of GNPs and SNPs. Fig. 1.A and B represent the clear absorption peak at 536 and 430 nm, which confirm the successful synthesis of gold and silver nanoparticles respectively. Fig. 1 C and D show the FTIR spectrum of the functional groups in the nanoparticles' surface. The absorption peaks (Fig. 1 C) of GNPs at 1705, 1639, 1219, and 1392 for the stretching vibrations C=O, C=C, C–O and the bending vibrations of –O–H confirm the successful creation of carboxyl

groups. As depicted in Fig. 1 D, aromatic C=C, aromatic C-H, and phenolic C-O were present at around 1624.06, 1465.90, and 1087.85 cm^{-1}, respectively. Aromatic C-H bending was detected at 713.66 and 860.25 cm^{-1}. The functional groups confirmed the presence of antibody on the electrode surface. The hydrodynamic average size and zeta potential of GNPs were determined to be 74.37 nm and −8.45, respectively (Fig. 1. E, G). Furthermore, the average hydrodynamic size (Fig. 1. F) and zeta potential of SNPs (Fig. 1 H) were found to be 116.9 nm and −5.59, respectively. The PDI result (0.26) represented a good GNPs stability and negative surface charges indicated the presence of carboxyl groups that stabilize the GNPs. The negative zeta potential of GNPs and SNPs helped to attach antibody to the electrode as electrostatic connection.

3.2. Electrochemical characterization of the immunosensor

The surface morphology of the electrode was investigated by scanning electron microscopy (SEM). Fig. 2.A illustrates the SEM images of the surface mucilage-GNPs-SNPs/GCE. The result of SEM showed that the electrode was well-modified. Fig. 2B demonstrates energy-dispersive X-ray spectroscopy (EDX). The results indicated the presence of different percentages of Au, Ag, N, O, and C at the composite electrode.

Typically, EIS was employed to study the interfacial characterization on different modified electrodes. The diameter of the semicircle is equal to the electron transfer resistance (R_{et}) and occurs in lower frequencies. R_{et} controls the electron transfer kinetics of the redox probe at the electrode interface which commonly shows faradaic process at the interface of electrode/electrolyte. An electrical circuit was depicted based on the features of the obtained impedance spectrum. The straight line of the Nyquist plots appeared at lower frequencies, which corresponds to the diffusion process of the electroactive species from solution to electrode interface (Warburg element, W) [23].

Herein, The Nyquist plots are displayed in Fig. 3A. The R_{et} value was obtained for a GCE 4367 Ω (curve a). The R_{et} value of mucilage/GCE increased from 4367 Ω to 773 s Ω (curve b). Once mucilage was utilized with a nanoparticle (gold or silver) separately (curve c & d), the R_{et} value of the electrode surface reduced. As could be seen in curve f, when gel was used with both nanoparticles (gold and silver), The R_{et} value significantly reduced. As a result, the presence of both particles, which assembled on the surface of electrode, provided the possibility of enhancing the conductivity of the mucilage.

Once Ab was incubated on the mucilage-GNPs-SNPs surface electrode, an increase was observed in the R_{et} value of the electrode (Fig. 3. A curve g) since the supporting on the electrode pre-

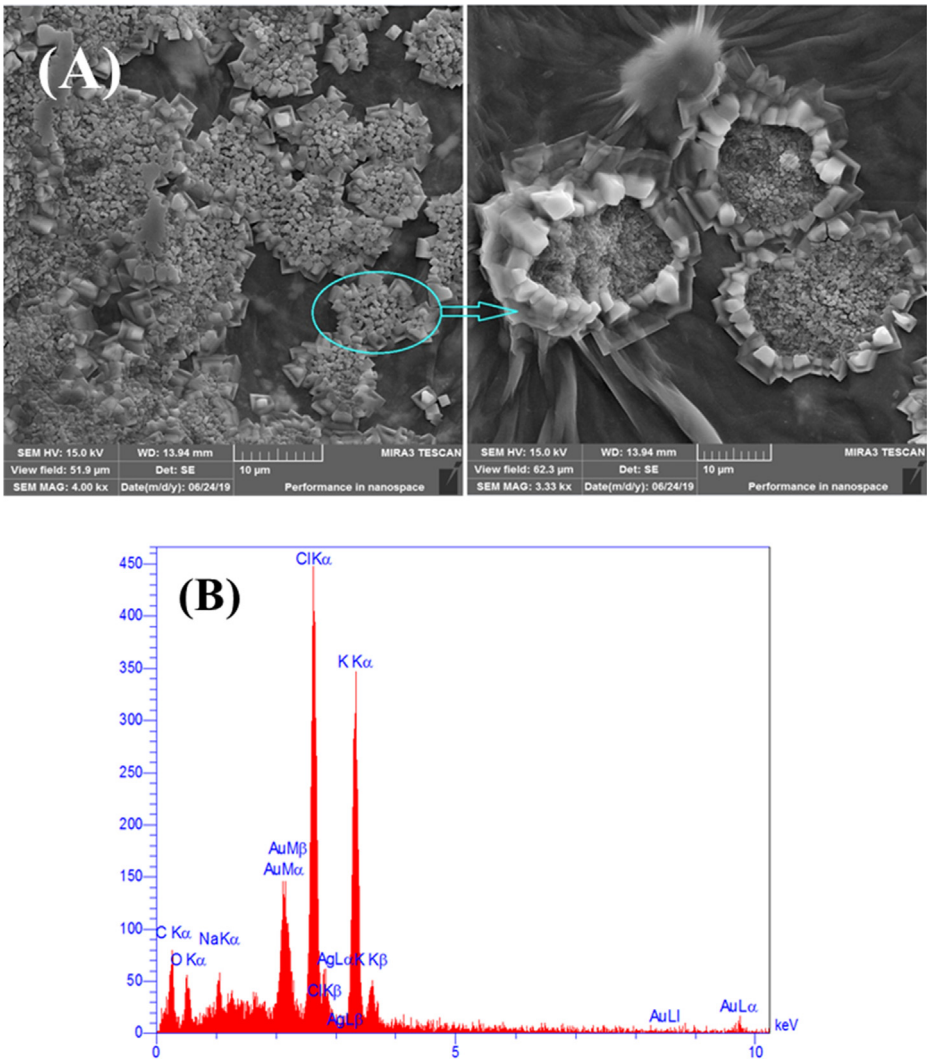

Fig. 2. SEM images of mucilage-GNPs-SNPs/GCE (A), Energy-dispersive X-ray spectroscopy of surface of the electrode (B).

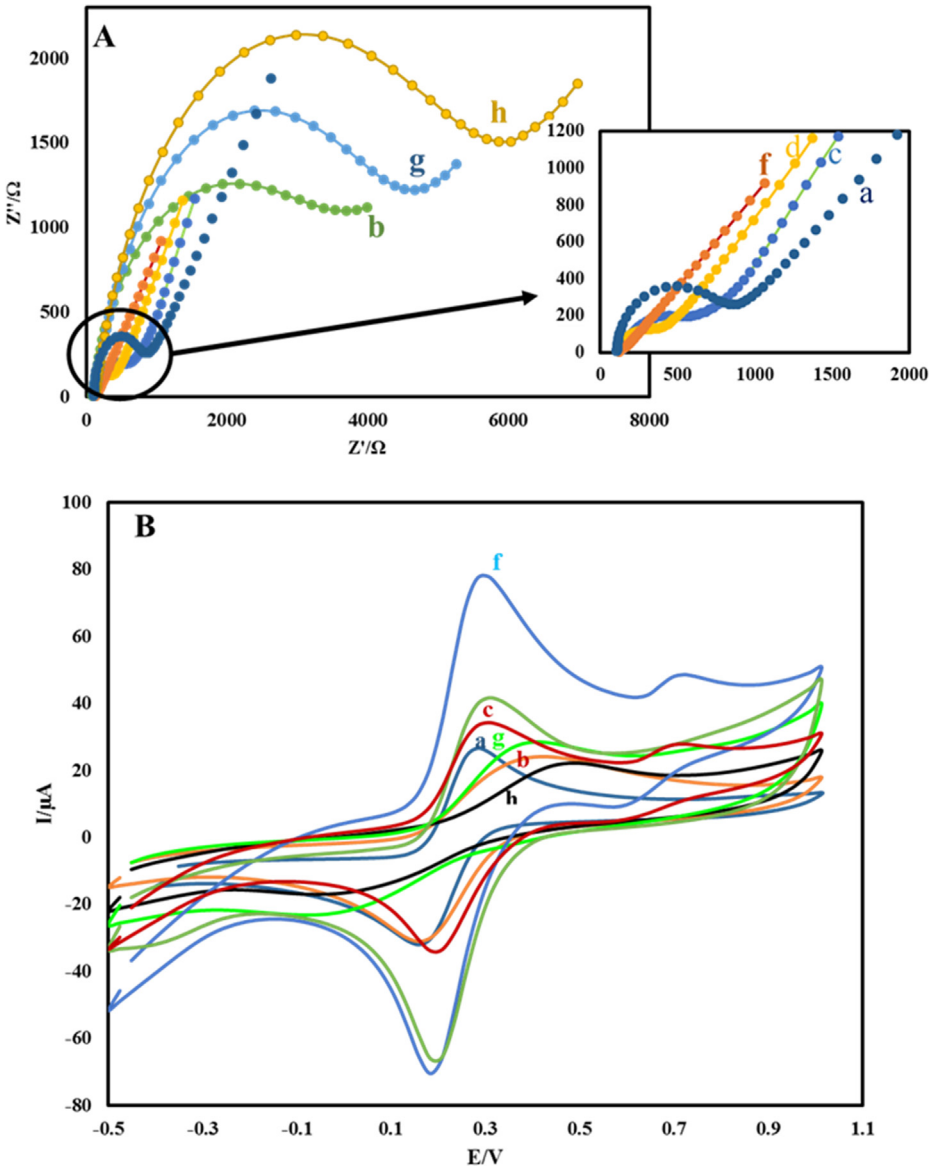

Fig. 3. Nyquist diagrams (A) and Cyclic voltammograms (B) of 0.1 M KCl solution containing 5.0 mM $K_3Fe(CN)_6^{3/4-}$ recorded at GCE (a), mucilage/GCE (b), mucilage-GNPs/GCE (c), mucilage-SNPs/GCE (d), mucilage-GNPs-SNPs/GCE (f), Ab/mucilage-GNPs-SNPs/GCE (g) and Ab-Ag/mucilage-GNPs-SNPs/GCE (h).

vents the redox $Fe(CN)_6^{3-/4-}$ on the electrode, which confirms the successfully incubation of Ab on the mucilage-GNPs-SNPs surface electrode. Following the incubation with PSA (10 ng/mL) on the GCE/ mucilage-GNPs-SNPs/Ab, the R_{et} value significantly increased (Fig. 3 A. curve h). This suggested that the PSA was successfully incubated with antibody.

For further investigation, the cycle voltammetry was used. Fig. 3.B shows cyclic voltammetry (CV) of $Fe(CN)_6^{3-/4-}$ at bare GCE (curve a), a well-defined redox peak. The peak current of the Fe $(CN)_6^{3-/4-}$ reduced at the mucilage/GCE surface (curve b) while it increased at the mucilage-GNPs/GCE and mucilage-SNPs/GCE (curve c & d). On the other hand, the redox current of the Fe $(CN)_6^{3-/4-}$ significantly increased when the electrode surface was modified with mucilage-GNPs-SNPs. A decrease was also observed in peak-to-peak separation (ΔE_p) (Fig. 4.B, curve f). The result clearly proved an increase in the mucilage's conductivity. The nanoparticles of the gold and silver increased surface to volume ratio in glass electrode, and due to the presence of functional groups in mucilage, the covalent bonds between them augmented the stability of Ab. The current value of the redox of $Fe(CN)_6^{3-/4-}$ on the surface Ab/mucilage-GNPs-SNPs/GCE significantly increased (curve g) in comparison with the CV of the non-immobilized electrode platform (curve g). The signal enhancement was ascribed to the physical coverage by the Ab and decrease in active surface area. The immunosensor was incubated with Ab in the presence of PSA for 40 min at room temperature, and its current value increased (curve h). It could confirm the formation of the Ab-PSA immune complex.

3.3. Optimization of experimental condition

To obtain high sensitivity and analytical performance immunosensor, we investigated effective parameters on the proposed immunosensor, such as the concentration/time of Ab included on an electrode and the incubation time of PSA with Ab.

The immobilization of Ab concentration was optimized and the solutions containing different concentrations of the Ab were immobilized on mucilage-GNPs-SNPs/GCE. Fig. 4.A represents the

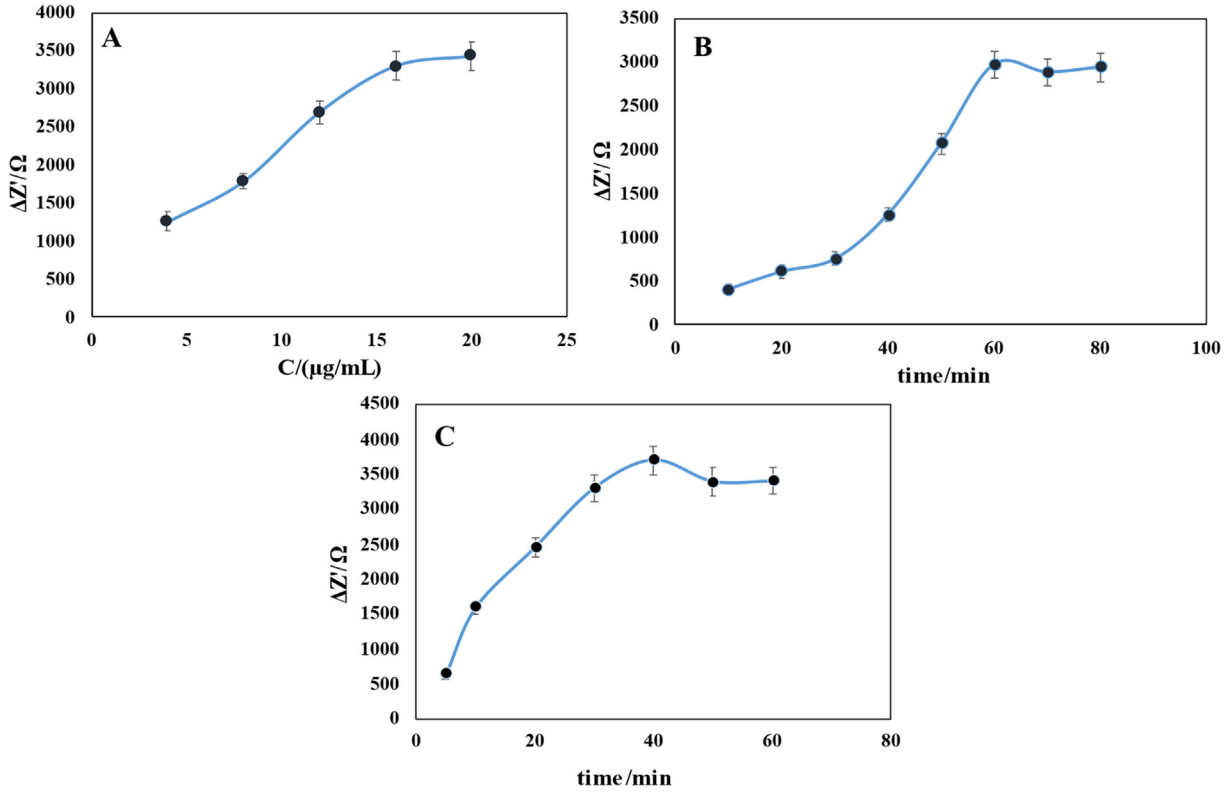

Fig. 4. Optimization of the experimental conditions: (A) the concentration of Ab, (B) the incubation time of Ab, (C) the incubation time of PSA whit Ab.

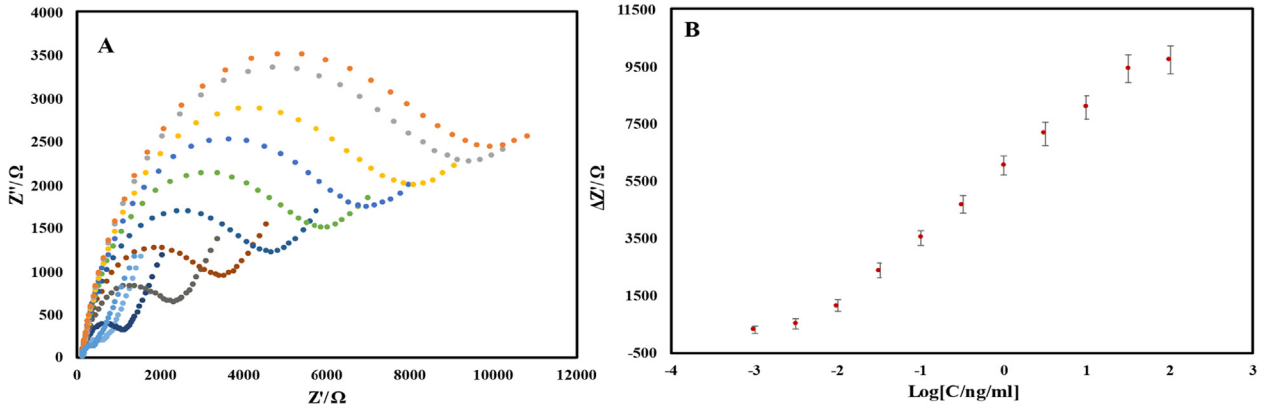

Fig. 5. EIS data of the developed immunosensor in pH = 7.4 PBS with different concentrations of PSA. Inset: The relationship between ΔRct and the concentrations of PSA. The error bars indicated the standard deviation of three-time measurements.

Table 1
The analytical performance of the prepared immunosensor.

Probe	Method	Liner range	Limit of detection	References
core–shell Au@Pt nanocrystals	DPV	0.1–50 ng mL^{-1}	0.018 ng mL^{-1}	[24]
NH_2-M-CeO_2	DPV& Amperometric	0.5 pg mL^{-1} to 50 ng mL^{-1}	0.16 pg mL^{-1}	[25]
core–shell AuPd@Au nanocrystals	DPV	0.1–50 ng mL^{-1}	0.078 ng mL^{-1}	[26]
Au/PANI	SWV	10 fg mL^{-1} to100 ng mL^{-1}	1.25 fg mL^{-1}	[27]
Au NPs	DPV	10 fg mL^{-1} to 100 ng mL^{-1}	3.3 fg mL^{-1}	[28]
rGO@AuNPs	DPV	0.1 to 100 ng mL^{-1}	0.08 ng mL^{-1}	[29]
Au@N-GQDs	Amperometric	0.01 pg mL^{-1} to 100 ng mL^{-1}	0.003 pg mL^{-1}	[30]
Ab1/AuNPs-ATPGO/GCE	DPV	0.01–1 pgmL^{-1}	3 fg mL^{-1}	[31]
Mucilage-GNPs-SNPs	EIS	0.1 pg mL^{-1} to 100 ng mL^{-1}	0.087 pg mL^{-1}	This work

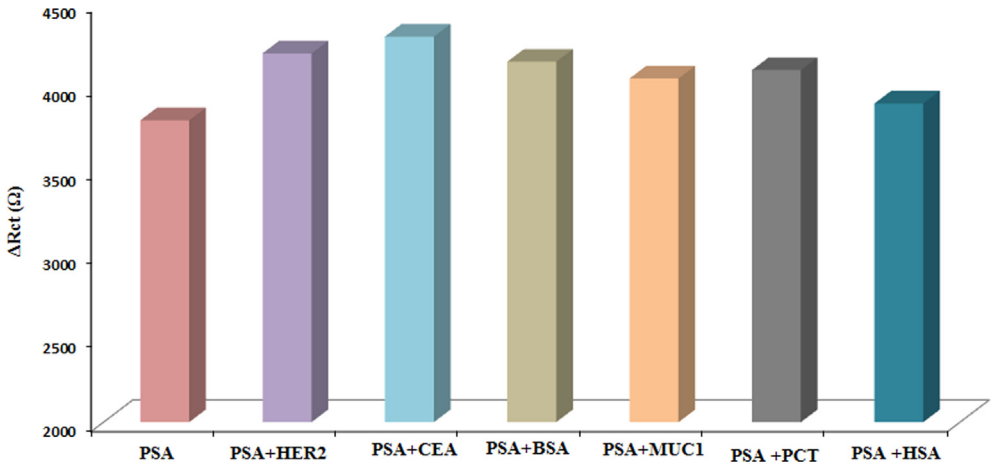

Fig. 6. The EIS responses of the immunosensor to 0.1 ng mL^{-1} PSA (A), 0.1 ng mL^{-1} PSA + 10 ng mL^{-1} HER2 (B), 0.1 ng mL^{-1} PSA + 10 ng mL^{-1} BSA (C) and 0.1 ng mL^{-1} PSA + 10 ng mL^{-1} MUC1 (D).

Table 2
Determination of PSA in human serum sample.

Sample	Added PSA concentration (ng mL^{-1})	Measured concentration by immunosensor (ng mL^{-1})	Recovery (%)
1	0.01	0.012	120.0
2	0.1	0.080	80.0
3	1	0.830	83.0
4	10	10.420	104.2

effect of the immobilization Ab concentration at the surface electrode modified with the current response. Consequently, the Ab concentration was optimized at 15 μg ml^{-1}, the highest current which allows the sensitive detection of PSA. The amount of over 15 μg ml^{-1} of Ab concentration was reduced. The incubation time played a pivotal role in sensor function since in a low incubation time, a weak connection was established between the Ab and the mucilage-GNPs-SNPs. Therefore, it was removed before the measurement. As shown in Fig. 4.B, the maximum signal of the measurement was observed at the incubation time of 60 min.

In order to use the maximum capacity of the immunosensor, the incubation different times between PSA and Ab were investigated. Fig. 4.C summarizes the results. The highest signal was observed at 40 min. Accordingly, 40 min was selected as the best incubation time between Abs and biomarkers.

3.4. Analytical performance

The analytical performance of the proposed immunosensor in the various concentrations of the PSA was assessed with EIS method. As shown in Fig. 5, the R_{et} increased proportionally with the increase in the biomarker concentration and the linear relationship was obtained between signal responses and the logarithmic biomarker concentration in the concentration range of 0.1 pg mL^{-1} to 100 ngmL^{-1}. The calibration curve with a regression equation of R/Ω = 2095.5Log [C_{PSA} /ngml^{-1}]$_+$ 5866.9 (R^2 = 0.988) and the detection limit (DL) were calculated based on $3S_b$ /m, where $3S_b$ is three times standard deviation of the blank signals and m is the slope of the calibration curve as 0.078 pgmL^{-1}.

The result implied that the analytical performance of the proposed immunosensor was perfectly done, and in comparison with other reported papers, there is further simplicity, higher sensitivity, and rapidity (Table 1).

3.5. Specificity of the immunosensor

The specificity of the presented immunosensor was investigated using HER2, CEA, MUC1, and BSA as the interference. Fig. 6 demonstrates the response of 10 ng mL^{-1} of interference solution with the 0.1 ng mL^{-1} of PSA. As could be seen, the signal interference was less than 10%, indicating that the specificity of the label-free electrochemical immunosensor was acceptable.

3.6. Human serum samples analysis

The accuracy in real blood samples were evaluated with the proposed electrochemical immunosensor. The serum samples were primarily collected from three healthy people. Subsequently, different concentrations of PSA were added into the samples. The standard addition method was applied to measure the PSA using EIS method. Table 2 represents the results. As it is obvious, the recovery of PSA was found between 80 and 120 %, which shows the good precision of the method for PSA monitoring with the proposed immunosensor. In other words, this electrochemical immunosensor provided a potential application for the analysis of PSA in real samples.

4. Conclusions

Since Quince seed mucilage, as a biopolymer, comprises different components, such as cellulose and water soluble polysaccharide, and due to the presence of L-arabinose, D-xylose and aldobiouric acids were applied as the electrode substrate for improving the electrode specific surface area, increasing the PSA antibody immobilization, and boosting the electrochemical efficiency of the electrode.

A new free-label electrochemical immunosensor was introduced for highly accurate detection of PSA based on novel green nanocomposites. In sensor architecture, the unique properties of mucilage-GNPs-SNPs were employed to stabilize the antibody. The immobilized antibody probe could efficiently track the biomarkers of PSA. The proposed immunosensor could respond with a wide linear range from 0.1 pg mL^{-1} to 100 ng mL^{-1}. The limit of detection was 0.087 pg mL^{-1}. In addition, the proposed sensor demonstrated good selectivity and stability. Accordingly, it can be utilized in medical clinics to quickly diagnose biomarkers.

Declaration of Competing Interest

The authors declare that they have no known competing financial interests or personal relationships that could have appeared to influence the work reported in this paper.

Acknowledgments

The authors gratefully acknowledge the research council of Kermanshah University of Medical Sciences (Grant Number. 97213) for financial support.

Compliance with ethical standards

The authors declare that they have no competing interests.

Declaration of Competing Interest

The authors declare that they have no conflict of interest.

References

[1] K.A. Cronin, A.J. Lake, S. Scott, R.L. Sherman, A.M. Noone, N. Howlader, et al., Annual report to the nation on the status of cancer, part I: National cancer statistics, Cancer (2018).
[2] K.A. Houston, J. King, J. Li, A. Jemal, Trends in prostate cancer incidence rates and prevalence of prostate specific antigen screening by socioeconomic status and regions in the United States, 2004 to 2013, J. Urol. (N. Y., NY, U. S.). 199 (2018) 676–82.
[3] C.E. Kyriakopoulos, Y.-H. Chen, M.A. Carducci, G. Liu, D.F. Jarrard, N.M. Hahn, et al., Chemohormonal therapy in metastatic hormone-sensitive prostate cancer: long-term survival analysis of the randomized phase III E3805 CHAARTED trial, J. Clin. Oncol. 36 (2018) 1080–1087.
[4] M.B. Kostova, W.N. Brennen, D. Lopez, L. Anthony, H. Wang, E. Platz, et al., PSA-alpha-2-macroglobulin complex is enzymatically active in the serum of patients with advanced prostate cancer and can degrade circulating peptide hormones, The Prostate (2018).
[5] F. Mollarasouli, V. Serafín, S. Campuzano, P. Yáñez-Sedeño, J.M. Pingarrón, K. Asadpour-Zeynali, Ultrasensitive determination of receptor tyrosine kinase with a label-free electrochemical immunosensor using graphene quantum dots-modified screen-printed electrodes, Anal. Chim. Acta. 1011 (2018) 28–34.
[6] F.S. Felix, L. Angnes, Electrochemical immunosensors – a powerful tool for analytical applications, Biosens. Bioelectron. 102 (2018) 470–478.
[7] L. Farzin, M. Shamsipur, Recent advances in design of electrochemical affinity biosensors for low level detection of cancer protein biomarkers using nanomaterial-assisted signal enhancement strategies, J. Pharm. Biomed. Anal. 147 (2018) 185–210.
[8] E. Arkan, G. Paimard, K. Moradi, A novel electrochemical sensor based on electrospun TiO2 nanoparticles/carbon nanofibers for determination of Idarubicin in biological samples, J. Electroanal. Chem. 801 (2017) 480–487.
[9] V.D. Krishna, K. Wu, D. Su, M.C. Cheeran, J.-P. Wang, A. Perez, Nanotechnology: review of concepts and potential application of sensing platforms in food safety, Food Microbiol. 75 (2018) 47–54.
[10] V. Kumar, S. Hebbar, A. Bhat, S. Panwar, M. Vaishnav, K. Muniraj, et al., Application of a nanotechnology-based, point-of-care diagnostic device in diabetic kidney disease, Kidney Int. Rep. 3 (2018) 1110–1118.
[11] M.L. Yola, N. Atar, A novel voltammetric sensor based on gold nanoparticles involved in p-aminothiophenol functionalized multi-walled carbon nanotubes: application to the simultaneous determination of quercetin and rutin, Electrochimica Acta 119 (2014) 24–31.
[12] M.L. Yola, N. Atar, T. Eren, H. Karimi-Maleh, S. Wang, Sensitive and selective determination of aqueous triclosan based on gold nanoparticles on polyoxometalate/reduced graphene oxide nanohybrid, RSC Adv. 5 (2015) 65953–65962.
[13] M.L. Yola, T. Eren, N. Atar, A sensitive molecular imprinted electrochemical sensor based on gold nanoparticles decorated graphene oxide: application to selective determination of tyrosine in milk, Sens. Actuat. B: Chem. 210 (2015) 149–157.
[14] M.L. Yola, T. Eren, N. Atar, H. Saral, İ. Ermiş, Direct-methanol fuel cell based on functionalized graphene oxide with mono-metallic and bi-metallic nanoparticles: electrochemical performances of nanomaterials for methanol oxidation, Electroanalysis 28 (2016) 570–579.
[15] M. Teimouri, F. Khosravi-Nejad, F. Attar, A.A. Saboury, I. Kostova, G. Benelli, et al., Gold nanoparticles fabrication by plant extracts: synthesis, characterization, degradation of 4-nitrophenol from industrial wastewater, and insecticidal activity–a review, J. Cleaner Prod. 184 (2018) 740–753.
[16] R. Shanmuganathan, D. MubarakAli, D. Prabakar, H. Muthukumar, N. Thajuddin, S.S. Kumar, et al., An enhancement of antimicrobial efficacy of biogenic and ceftriaxone-conjugated silver nanoparticles: green approach, Environ. Sci. Pollut. Res. 25 (2018) 10362–10370.
[17] T. Abdelghany, A.M. Al-Rajhi, M.A. Al Abboud, M. Alawlaqi, A.G. Magdah, E.A. Helmy, et al., Recent advances in green synthesis of silver nanoparticles and their applications: about future directions. A review, BioNanoScience 8 (2018) 5–16.
[18] N. Elahi, M. Kamali, M.H. Baghersad, Recent biomedical applications of gold nanoparticles: a review, Talanta (2018).
[19] A.E. Al-Snafi, The medical importance of Cydonia oblonga – a review, IOSR J. Pharm. 6 (2016) 87–99.
[20] B.M. Silva, P.B. Andrade, P. Valentão, F. Ferreres, R.M. Seabra, M.A. Ferreira, Quince (Cydonia oblonga Miller) fruit (pulp, peel, and seed) and Jam: antioxidant activity, J. Agric. Food Chem. 52 (2004) 4705–4712.
[21] M.A. Hussain, G. Muhammad, M.T. Haseeb, M.N. Tahir, Functional Biopolymers. (2019) 1–22.
[22] M. Hamad, H. Mohammed, M. Merdaw, Ibn AL-Haitham Journal For Pure and Applied Science. 24 (2017).
[23] Z.L. H. Huang, X. Yang, Anal, Application of Electrochemical Impedance Spectroscopy for Monitoring Allergen-Antibody Reactions Using Gold Nanoparticle-Based Biomolecular Immobilization Method Anal Biochem. 356 (2006) 208–14.
[24] R. Wang, A.-J. Wang, W.-D. Liu, P.-X. Yuan, Y. Xue, X. Luo, et al., A novel label-free electrochemical immunosensor for ultra-sensitively detecting prostate specific antigen based on the enhanced catalytic currents of oxygen reduction catalyzed by core-shell Au@ Pt nanocrystals, Biosens. Bioelectron. 102 (2018) 276–281.
[25] Y. Wei, X. Li, X. Sun, H. Ma, Y. Zhang, Q. Wei, Dual-responsive electrochemical immunosensor for prostate specific antigen detection based on Au-CoS/graphene and CeO2/ionic liquids doped with carboxymethyl chitosan complex, Biosens. Bioelectron. 94 (2017) 141–147.
[26] R. Wang, W.-D. Liu, A.-J. Wang, Y. Xue, L. Wu, J.-J. Feng, A new label-free electrochemical immunosensor based on dendritic core-shell AuPd@ Au nanocrystals for highly sensitive detection of prostate specific antigen, Biosens. Bioelectron. 99 (2018) 458–463.
[27] D. Zhang, W. Li, Z. Ma, Improved sandwich-format electrochemical immunosensor based on "smart" SiO2@ polydopamine nanocarrier, Biosens. Bioelectron. 109 (2018) 171–176.
[28] M. Li, P. Wang, F. Pei, H. Yu, Y. Dong, Y. Li, et al., A novel signal amplification system fabricated immunosensor based on Au nanoparticles and mesoporous trimetallic PdPtCu nanospheres for sensitive detection of prostate specific antigen, Sens. Actuat. B. 261 (2018) 22–30.
[29] X. Liu, D. Wang, J. Chu, Y. Xu, W. Wang, Sandwich pair nanobodies, a potential tool for electrochemical immunosensing serum prostate-specific antigen with preferable specificity, J. Pharm. Biomed. Anal. (2018).
[30] Y. Yang, Q. Yan, Q. Liu, Y. Li, H. Liu, P. Wang, et al., An ultrasensitive sandwich-type electrochemical immunosensor based on the signal amplification strategy of echinoidea-shaped Au@ Ag-Cu_2O nanoparticles for prostate specific antigen detection, Biosens. Bioelectron. 99 (2018) 450–457.
[31] Hilal Medetalibeyoglu, Gül Kotan, Necip Atar, Mehmet Lütfi Yola., A novel and ultrasensitive sandwich-type electrochemical immunosensor based on delaminated MXene@AuNPs as signal amplification for prostate specific antigen (PSA) detection and immunosensor validation, Talanta, 20 (2020).